The University of Rhode Island, Kingston, RI 02881-0817
Department of Physics, College of Arts and Sciences (401) 792-2633

August 4, 1986

NASA Scientific and Technical
Information Facility
Post Office Box 8757
Baltimore and Washington
International Airport, MD 21240

Gentlemen:

A progress report on our research efforts covering NASA Grant No. NAG-1-519 is enclosed. This report summarizes our activities from October 1, 1985 to June 30, 1986.

A final report describing in detail our yearly efforts will be submitted upon completion of the report period.

Sincerely,

Frank W. Cuomo
Professor of Physics

bg
enclosure

C: Dr. Allan Zuckerwar
NASA Langley Research Center

The University of Rhode Island

Physics Department

Progress Report No. 2

(October 1, 1985 - June 30, 1986)

Contract No. NAG-1-519

NASA Langley Research Center
Hampton, VA

"Fiber Optic Pressure Sensors in Skin-Friction Measurements"

by

Frank W. Cuomo

August 4, 1986

SUMMARY OF RECENT EFFORTS (October 1, 1985 - June 30, 1986)

The intent of this research is to investigate the utilization of a fiber optical lever in the design and construction of a pressure sensor of minimal dimensions devoted to the measurement of shear motion associated with skin-friction measurements. In addition, with suitable design modifications, the sensor can be adapted to the measurement of normal pressures. The following comments summarize our activities on this project during the period given above.

The first on-site test in a 7" x 11" low speed wind tunnel was held by URI personnel at the NASA-Langley Research Center on August 12-16, 1985. This test was designed to establish the behavior of optical fiber pressure and shear stress sensors in a wind tunnel environment. The targeted goal was to detect minimum pressures on the order of 10^{-5} PSI. The results of this first test were partially conclusive; and upon its completion, the following action items were agreed upon by LaRC and URI to improve the sensitivity and signal to noise ratio of these probes for future experimentation.

1. The area of the fibers will be increased, either through increased diameter or greater number of fibers. This will necessitate redimensioning and remachining the probes. The machining will be done at LaRC.
2. A specification will be added concerning the centerlines of the hole and threads of the fiber probe holder. These should be paralleled to within 1/2 degree for required fiber alignment. The fit of the thread will be changed from class 3 to class 2.
3. The elastomer will be changed to one having a lower modulus of elasticity. A possible candidate is RTF760.
4. The design of a schlieren shear probe will be considered.
5. An attempt will be made to reduce the electrical noise in the supporting electronics.
6. The length of the probes will be redimensioned to fit the 7" x 11" tunnel along the entire test section.

Our efforts since October 1985 have been directed toward the implementation of these proposed revisions, and we are presently preparing for a second test to be held at the same location at LaRC on August 18-22, 1986, incorporating the following changes and/or additions:

1. The optical fiber core diameters and number of fibers have been increased for the pressure sensors. We now have two new pressure probe designs which incorporate seven optical fibers. The first consists of one 400-micron core transmit fiber surrounded by six 400-micron core receive fibers. The second design consists of one 400-micron transmit fiber surrounded by three 400-micron and three 100-micron receive fibers which will provide the ratio output measurements. These changes did not affect the overall dimensions of the original sensor bodies but only a slight increase in the inside diameter of the hypodermic needles.
2. The three-fiber arrangement previously used for the shear sensors was retained, but the fiber core diameters were increased to one 400-micron transmit fiber and two receive fibers consisting of one 400- and one 100-micron core dimensions.
3. To further improve device sensitivity, another approach, supplementing the use of soft elastomers, includes elements consisting of metallized polyester film. This concept has been implemented, and present projections indicate increased displacement sensitivity.
4. A followup to the above changes has been the completion of new computer models to predict the sensitivity of these new devices.
5. The electronic package has been revised to include a zero offset, new photodetectors and lower noise characteristics.
6. Improved calibration methods have been devised and implemented to improve the D.C. and A. C. calibration of the sensors prior to testing.

A paper related to this work was recently presented at the SPIE International Symposium in Quebec City, Canada, as indicated under references below. A copy of the paper is enclosed.

REFERENCES

I. Cuomo, F. W., Kidwell, R. S., Hu, A. "A Fiber Optic Sensor Sensitive to Normal Pressure and Shear Stress," Proceedings of the SPIE 1986 Quebec International Symposium on Optical and Optoelectronic Applied Sciences and Engineering, Quebec City, Canada, June 1986.

A fiber optic sensor sensitive to normal pressure and shear stress

Frank W. Cuomo

Department of Physics, University of Rhode Island, Kingston, R.I. 02881
and
Naval Underwater Systems Center, Newport, R.I. 02841

Robert S. Kidwell

Department of Physics, University of Rhode Island, Kingston, R.I. 02881

and

Andong Hu

Department of Physics, University of Rhode Island, Kingston, R.I. 02881

Abstract

A fiber optic lever sensing technique that can be used to measure normal pressure as well as shear stresses is discussed. This method uses three unequal fibers combining small size and good sensitivity. Static measurements appear to confirm the theoretical models predicted by geometrical optics and dynamic tests performed at frequencies up to 10 kHz indicate a flat response within this frequency range. These sensors are intended for use in a low speed wind tunnel environment.

Introduction

Several experimental methods are available for the measurement of skin friction. A brief review of these methods is given by Brown and Joubert.[1] They include the momentum techniques, the wall similarity techniques, direct measurements and dye traces. Within the wall similarity techniques are included velocity profile methods, heat transfer methods and similarity of flow about obstacles, which have utilized static pressure holes, boundary-layer fence, Preston tubes, Stanton tubes and razor blade techniques. The principle of determining the wall shear stress by direct measurements implies cutting from the wall a small elemental piece and mounting it in such a way that it can move freely in the stream direction and thus measure the force acting upon it. This approach, which has been referred to as the floating-element method, has been utilized. For example, Brown and Joubert, Frei and Thomann,[2] and McAllister, Pierce and Tennant[3] have applied the floating element concept in some form to the experimental determination of skin friction in the turbulent boundary layers. When pressure gradients are present along a surface acted upon by unsteady flows, it is also possible to establish the wall shear stress by the direct measurement of pressures at different points on the surface. Pressure fluctuations at a solid surface can be determined without flow disturbance by fitting a gauge flush with the surface. Richards[4] discusses several types of devices useful in the measurement of unsteady pressure and forces. The relevant parameters of these devices include a) sensitivity, b) frequency response, c) size, d) dynamic range and linearity, e) calibration and f) sensitivity to other forces due to structural vibrations, etc. Since all of these parameters dictate how well a transducer will operate in a particular environment, it is important that each be given full attention. As indicated by Reynolds,[5] condenser microphones and piezo-electric crystals have been often used because of their broad and flat frequency response (20 Hz - 40 kHz). Spatial resolution, however, is a problem because these devices, due to their size, will not be sensitive to small-scale fluctuations such as found near a solid wall. The intent of this paper is to describe the application of a fiber optic pressure sensor which can be effectively utilized to obtain normal and shear forces acting along a solid surface due to turbulent fluid flow parallel to this surface. The dimensions of the device are such that the sensing element will provide the measurement of small-scale fluctuations and will be flush with the solid surface without introducing perturbations to the flow due to its presence (no gaps necessary). Its small size will also permit the detection of small-scale pressure fluctuations in the vicinity of the solid wall. Its frequency response will extend into the kilohertz range and will possess acceptable linearity and dynamic range for its intended application.

The minute dimensions of the fiber optic device prohibit the use of interferometric sensors due to their complexity and projected size. However, several candidates, which utilize intensity modulation techniques, can be applied to sensor designs useful for this application. In particular, the fiber optic lever has been suggested as a possible choice

due to its small dimensions, ease of construction and adaptability. Non-contacting fiber optic levers have been described for a range of applications including pressure transducers, pressure and pressure gradient hydrophones and shock measurements.[6,7,8,9] Lawson and Tekippe[9] measured pressure using diaphragm curvature. Their method related diaphragm curvature to the ratio of light intensity received by two sets of fibers concentric with the source fibers. Using the ratio of received intensity compensates for input power variations, as well as fiber and coupling losses. All fibers were of equal core diameters. McMahon et al.[10] describe a hydrophone based on the photoelastic effect, which also uses an output ratio method. Cuomo[11] describes a technique, which uses only three fibers, one transmit and two receive, of unequal core dimensions. Light is reflected from a diaphragm and is collected by the two receive fibers, with the ratio of their outputs determining the sensitivity. He uses a geometric determination of the illuminated areas of the receive fibers to predict sensitivities as a function of fiber-reflector gap. Use of unequal receive fiber core diameters results in improved sensitivities which permit the consideration of such a small number of fibers in the sensor.

Analytical models

It has been shown[11] that it is possible using geometrical optics to obtain an approximation to device sensitivity for the case of a reflector whose motion is normal to the fiber ends. Similarly, sensitivities can be approximated for reflector motion parallel to the fiber ends. In either case it is unnecessary to consider optical fiber losses, reflectivity losses and similar factors. Thus, one can describe a related method which uses the same three-fiber arrangement, but is sensitive to shear stress rather than pressure. While other sensors have used a diaphragm undergoing normal motion relative to the fiber ends, shear motion can be detected by employing a floating element reflective only on half the area illuminated by the transmit fiber. Motion parallel to the fiber ends is then translated directly into modulation of the output light intensity of the receive fibers. A geometrical optics method is used to predict sensitivities. Our data indicate the feasibility of a sensor of this type. Table 1 below provides the optical fiber specifications used for both normal and shear motion.

Table 1.

Fiber	Core Diameter (microns)	Cladding Diameter (microns)	Numerical Aperture
Transmit	200	240	0.30
Receive (A)	200	240	0.30
Receive (B)	52	125	0.21

Figure 1 shows the basic sensor configuration with the reflector arranged for motion normal to the distal end while Figure 2 shows the illuminated areas of the two receive fibers as a function of reflector distance from the fiber surface. The sensitivity of the sensor is the change in the ratio of the two areas per unit displacement. This sensitivity is shown in Figure 3. Similar results are obtained for motion parallel to the distal end as illustrated in Figure 4 by the cross-section of three adjacent step-index fibers. Reflected back on the plane of the fiber surfaces is the area of illumination due to the transmit fiber. This area varies with the fiber-reflector distance but for a sufficiently large distance a fully reflecting element would completely illuminate both receive fibers as shown. Only part of the illuminated region of the reflector is reflective. A straight line marks the edge of the reflective portion. The remaining portion of the reflector is assumed non-reflective, with the result that the illuminated areas on the receive fibers depend on the parallel reflector displacement. The figure shows the resulting illuminated areas A and B of the large and small receive fibers and the total area of illumination due to the transmit fiber. For simplicity Figure 4 illustrates three fibers of equal numerical aperture, but the model easily accommodates different numerical apertures for the three fibers. This model can be used to determine optimum choices of transmit and receive fiber core and cladding diameters, the distance between fiber centers and numerical apertures. Data were generated using this model, with the fiber parameters given in Table 1. Figure 5 shows the illuminated areas of the receive fibers as a function of reflector displacement. The reflector displacement is referenced to the center line of the transmit fiber. Figure 6 shows the ratio sensitivity. The model predicts remarkably high values for sensitivity. In addition, the optimum fiber to reflector distance is quite large, making design requirements less exacting.

Experimental methods

To test the models, prototype sensors were constructed. Three commercially available step-index glass fibers were assembled in a short metal sheath. An ultrathin front surface mirror was used as the reflector. For shear motion, the mirror edge provided the reflective to non-reflective edge. The light source was a Motorola MFOE1201 LED with a peak wavelength of 820 nm, and two UDT FO-02 400 photodiodes were used for detection. For static tests, the source was voltage modulated with a square wave and the photodiode outputs filtered (1 Hz

band) through lock-in amplifiers. For these tests, the output ratio was calculated from the separate output signals. Static displacement tests were made for both longitudinal and shear motion to confirm the sensor operation as predicted by Figures 2, 3, 5 and 6. Mirror displacements normal and parallel to the fiber end were made using a micrometer having a resolution of 0.025 microns and the fiber-reflector gap was chosen to maximize the total light throughput. Figures 7 and 8 are the experimental results for the longitudinal predictions of Figures 2 and 3 while Figures 9 and 10 provide similar results comparable to Figures 5 and 6. The AC response of the sensors was obtained for frequencies up to 10 kHz. The test consisted of attaching a mirror to the head mass of a piezo-electric transducer in such a way as to provide either longitudinal or shear motion relative to a fiber probe which was positioned at a nominal distance (and lateral position in the shear case) determined from the DC sensitivity curves. For the longitudinal test, a probe-mirror distance of 238 μm was chosen, while the shear test was performed at a mirror distance of 760 μm and a lateral position of 62 μm referenced to the centerline of the transmit fiber. The transducer is driven by a B & K 1022 oscillator at 100 volts (RMS). The output of the photodiode amplifier is fed into an Ithaco lock-in amplifier with a 1 Hz bandwidth. The transducer driving frequency is also used as the reference frequency for the lock-in amplifier. Thus, by varying the oscillator frequency, the range from 20 Hz to 10 kHz (the maximum frequency range of the lock-in) can be scanned with a constant bandwidth. In order to establish the frequency dependence of the transducer, a commercial piezo-electric accelerometer was mounted in place of the mirror on the transducer face and the output of the accelerometer recorded as a function of frequency. Figure 11 shows the AC response of the large and small receive fibers for the normal configuration, while Figure 12 provides the ratio response. Similarly, Figures 13 and 14 show the results of the shear data. The response of the accelerometer was converted into displacement assuming the relationship $x = a/\omega^2$, where a is the acceleration, x is the displacement and ω is the angular frequency. Figure 15 is the calculated displacement from the accelerometer showing good agreement with the probe data. This indicates no frequency dependence in the probes themselves in this range. Structure common to all of the curves can be assumed to be resonances of the transducer. It is noted that the frequency range shown in Figures 11 through 15 is given in Hertz. Finally, a static pressure test was performed at the University of Rhode Island to characterize the performance of the sensors at pressures larger than those encountered in a wind tunnel environment. The factors of interest in this test were the magnitude and linearity of response of the pressure sensors in the higher pressure range up to 0.36 psi. Figure 16 shows the output change of the two fibers of the pressure sensor, which exhibit the desired linearity of response. Figure 17 provides the change in the ratio of the two outputs shown in Figure 16.

Conclusions

It is found that optical fiber sensors of the lever type can be used for the measurement of normal and shear forces such as found in a wind tunnel environment. The minute sensor dimensions lend themselves to the design of small floating element assemblies which provide the direct analysis of skin friction. This work was supported by the NASA Langley Research Center, Hampton, VA, and the Naval Underwater Systems Center, Newport, RI.

References

1. Brown, K. C., and Joubert, P. N., "The Measurement of Skin Friction in Turbulent Boundary Layers with Adverse Pressure Gradients," J. Fluid Mech., Vol. 35, pp. 737-757. 1969.

2. Frei, D., and Thomann, H., "Direct Measurements of Skin Friction in Turbulent Boundary Layer with a Strong Adverse Pressure Gradient," J. Fluid Mech., Vol. 101, pp. 79-95. 1980.

3. McAllister, J. E., Pierce, F.J., and Tennant, M. H., "Preston Tube Calibrations and Direct Force Floating Element Measurements in a Two-Dimensional Turbulent Boundary Layer," J. Fluids Eng., Vol. 104, pp. 156-160. 1982.

4. Richards, B. E., "Measurement of Unsteady Fluid Dynamic Phenomena," von Karman Institute for Fluid Dynamics, Hemisphere Publishing Corp., Washington, DC, Chap. 3. 1977.

5. Reynolds, A. J., "Turbulent Flows in Engineering," John Wiley & Sons, New York, NY, Chap. 2. 1974.

6. Kobayashi, K., Okuyama, H., Kato, T., and Yasuda, T., "Fiberoptic Catheter-Tip Micromanometer," J. J. Med. Electron, Biol. Eng., Vol. 15, pp. 25-32. 1977.

7. Cook, R. O., Hamm, C. W., and Akay, A., "Shock Measurement with Non-Contacting Fiber Optic Levers," J. Sound Vib., Vol. 76, pp. 443-456. 1981.

8. Cuomo, F. W., "Pressure and Pressure Gradient Fiber Optic Lever Hydrophones," J. Acoust. Soc. Am., Vol. 73, pp. 1848-1857. 1983.

9. Lawson, C., and Tekippe, V. J., "Fiber-Optic Diaphragm-Curvature Pressure Transducer," Opt. Lett., Vol. 8, pp. 286-288. 1983.

10. McMahon, D. H., Soref, R. A., and Sheppard, L. E., "Sensitive Fieldable Photoelastic Fiber-Optic Hydrophone," J. Lightwave Technol., Vol. LT-2, pp. 469-478. 1984.

11. Cuomo, F. W., "The Analysis of a Three-Fiber Lever Transducer," Proceedings of the SPIE Technical Symposium, Vol. 478, pp. 28-32. 1984.

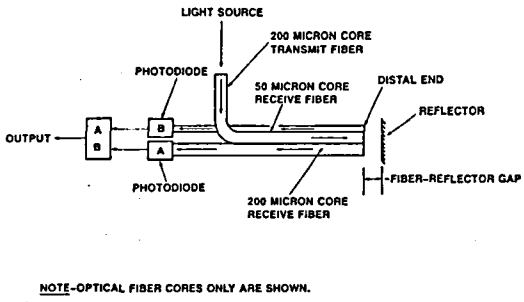

Figure 1. A three-fiber lever transducer. Longitudinal motion.

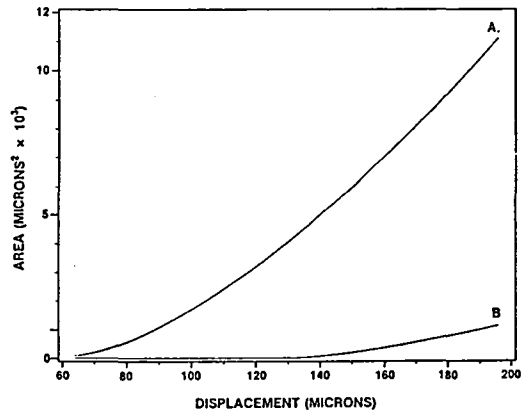

Figure 2. Illuminated areas of 200 and 50 μm receive fibers. Longitudinal motion.

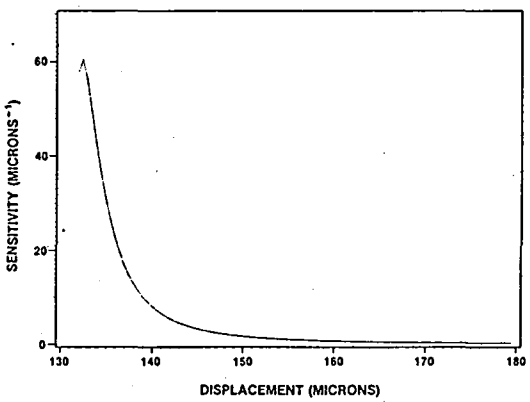

Figure 3. Predicted sensitivity of three-fiber sensor. Longitudinal motion.

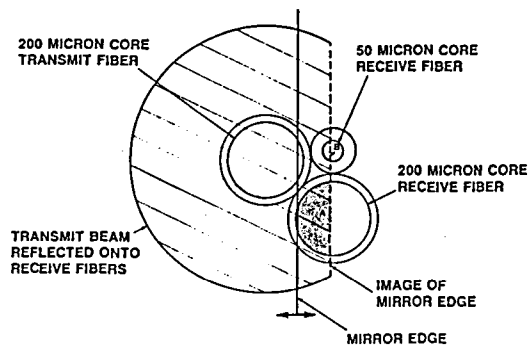

Figure 4. Distribution of transmit and receive fibers at distal end. Shear motion.

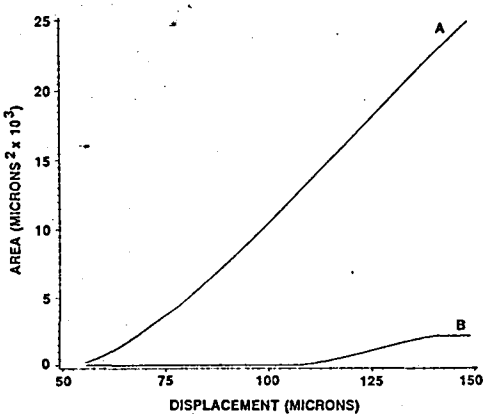

Figure 5. Illuminated areas of 200 and 50 μm receive fibers. Shear motion.

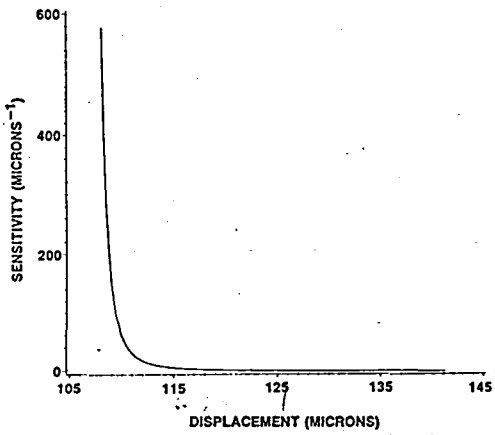

Figure 6. Predicted sensitivity of three-fiber sensor. Shear motion.

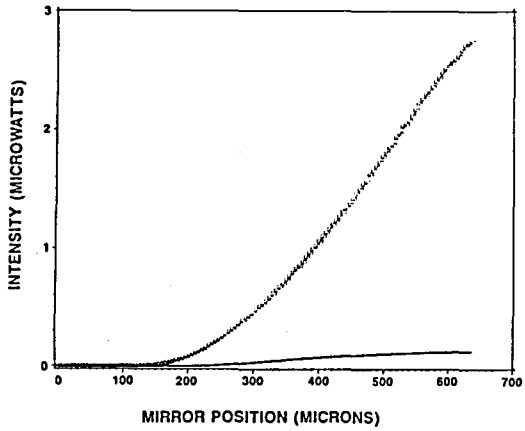

Figure 7. Experimental data of 200 and 50 μm receive fibers. Static longitudinal measurements.

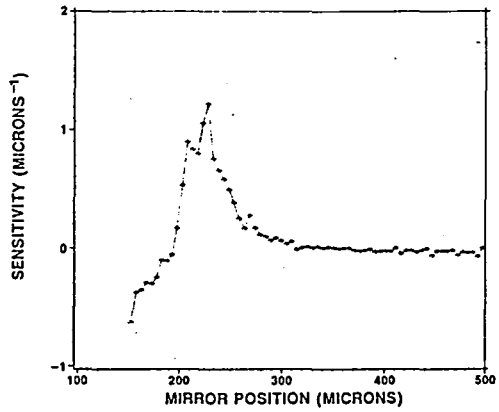

Figure 8. Experimental data of D.C. sensitivity. Longitudinal motion.

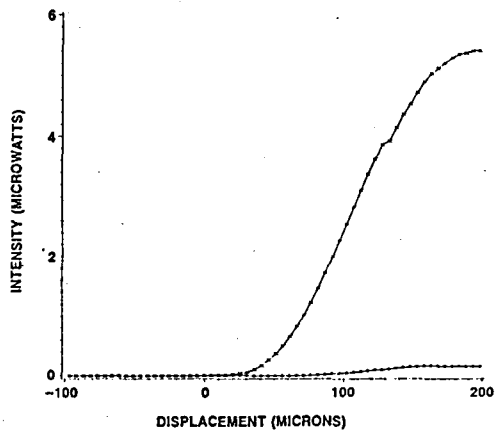

Figure 9. Experimental data of 200 and 50 μm receive fibers. Static shear measurements.

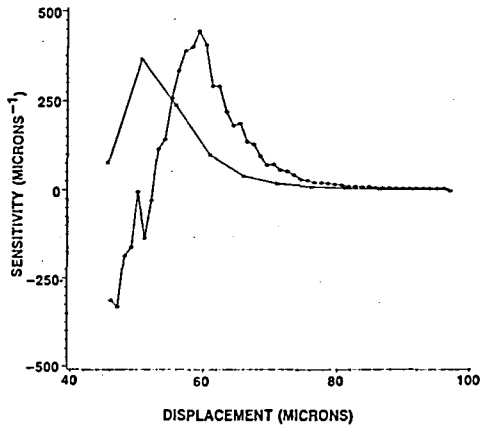

Figure 10. Experimental data of D.C. sensitivity. Shear motion. Right peak at 1μm intervals, left peak at 5μm intervals.

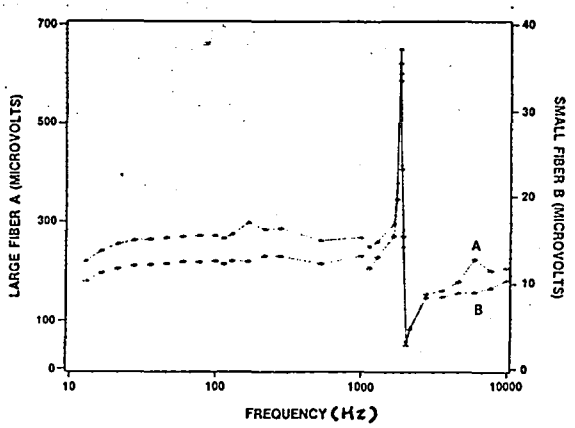

Figure 11. Experimental data of 200 and 50 μm receive fibers. Dynamic longitudinal measurements.

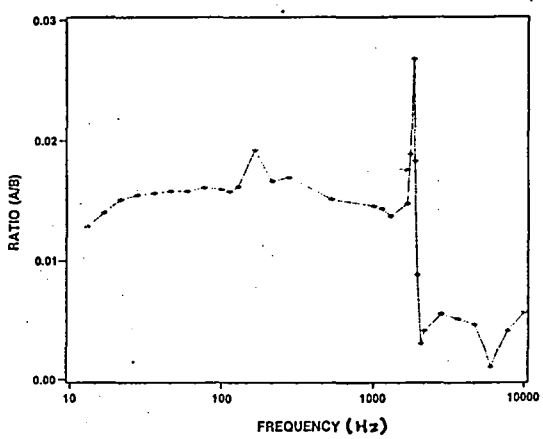

Figure 12. Experimental data of A.C. sensitivity. Longitudinal motion.

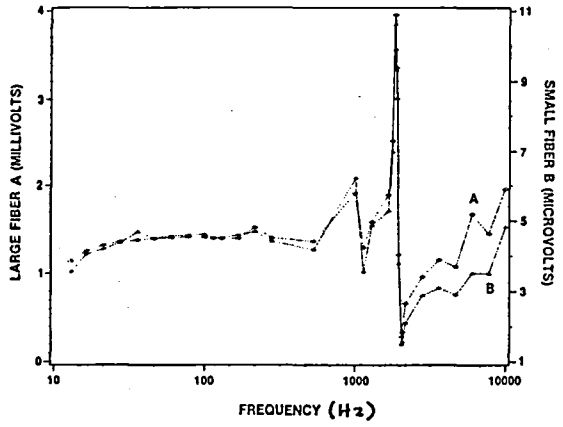

Figure 13. Experimental data of 200 and 50 μm receive fibers. Dynamic shear measurements.

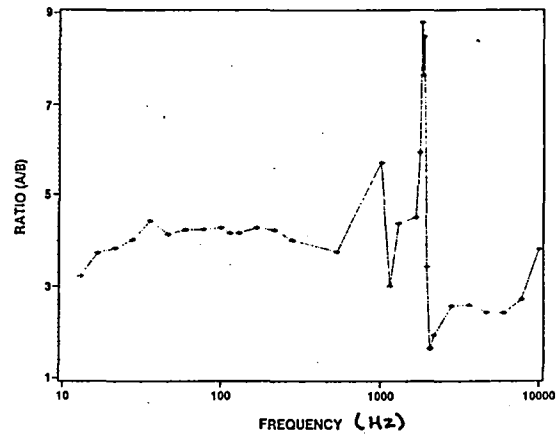

Figure 14. Experimental data of A.C. sensitivity. Shear motion.

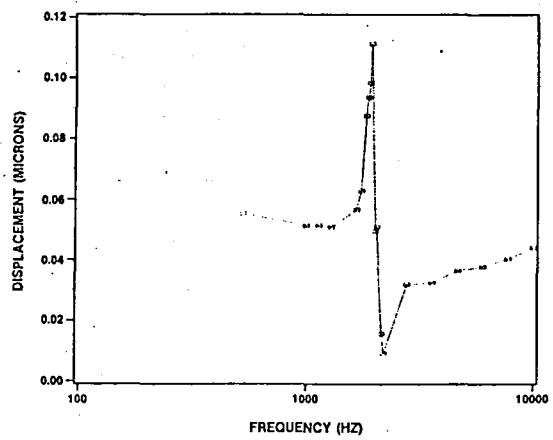

Figure 15. Experimental displacement of accelerometer near resonance.

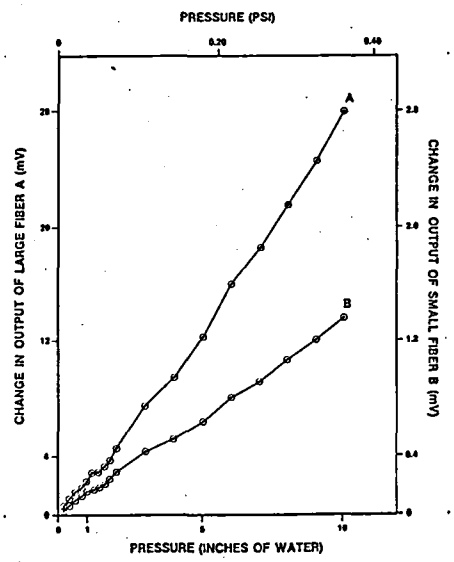

Figure 16. Static pressure measurements of 200 and 50 μm receive fibers.

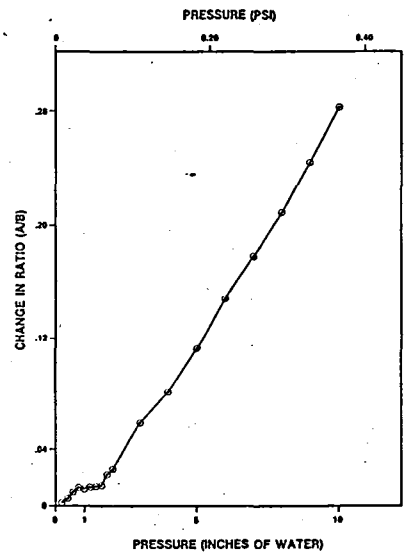

Figure 17. Change in ratio of receive fibers for static pressure measurements.

End of Document